Hindawi
Advances in Mathematical Physics
Volume 2022, Article ID 5258035, 9 pages
https://doi.org/10.1155/2022/5258035

Research Article

Dynamical Features of Isolated Two- and Three-Level Atoms Interacting with a Cavity Field

M. Y. Abd-Rabbou,[1] **E. M. Khalil**,[2] **and Fadhel Almalki**[2]

[1]*Mathematics Department, Faculty of Science, Al-Azhar University, Nasr City, 11884 Cairo, Egypt*
[2]*Department of Mathematics, College of Science, Taif University, P.O. Box 11099, Taif 21944, Saudi Arabia*

Correspondence should be addressed to M. Y. Abd-Rabbou; m.elmalky@azhar.edu.eg

Received 20 February 2022; Revised 14 June 2022; Accepted 27 June 2022; Published 21 July 2022

Academic Editor: Sandro Wimberger

Some dynamical features of two- and three-level atoms interacting locally with an ideal cavity field are investigated. These dynamical features are introduced by employing the statistical atomic inversion, entropy squeezing, and tomographic entropy. Our results show that the initial setting states play an essential role in the temporal evolution of the three quantities. The sensitivity of the two-level atomic state is less than that depicted by the three-level atom. The initial state has a small impact on the two types of entropies for the two-level atom. However, it has an appreciable effect in the case of the three-level atom for different regulations of the initial atomic state.

1. Introduction

The interaction between different substances is still a hot topic in quantum optics and information issues. These issues concern the linear atom-field interaction [1] and nonlinear atom-field interaction [2]. The classical simulation of nonlinear atom-field interaction in photonic lattices has been realized [3]. In the ultra-strong coupling regime, the quantum simulation by applying a rotating wave approximation for the light-matter interaction has been introduced [4]. Some theoretical and practical phenomena of field-atom interaction, such as entanglement, revival, and collapse have been explained [5]. The entanglement of field-field interaction has been addressed [6]. Moreover, the effect of cross-Kerr nonlinear on the decoherence of a quantum system was studied [7]. The entanglement of time-dependent atom-atom interaction was discovered [8]. Some conical transformations are used to handle the atom-atom interaction with the presence of time dependence. For these interactions, some statistical and quantum information has been illustrated to analyze different phenomena [9]. Among these phenomena is the quantum entanglement [10], which is a cornerstone of quantum information theory [11]. Via employing the von Neumann entropy, the degree of entanglement has been studied for different substances, such as the entanglement of atom-field interaction in resonance and off-resonance cases, has been explored [12]. The degree of entanglement has also been discussed under the Unruh effect, for the two-qubit [13], qubit-qutrit [14], and two-qutrit [15]. Furthermore, the dynamics of entanglement of two isolated Jaynes-Cummings Hamiltonian have been studied, where the first atom interacting only with one cavity field and the second atom interacting with another cavity [16]. In addition, the entanglement of linear atom-field interaction has been illustrated under the influence of Kerr-like medium [17], degenerate parametric amplifier [18], vibrating graphene membrane [19, 20], external classical field [21], damping terms [22], Stark shift terms [23], and deformed cavity field [24]. A double Jaynes-Cummings models in the presence of non-Markovian environments [25], and Kerr medium [26] have been developed to simulate the entanglement dynamics. For high-dimensional atomic

systems, the exact solution of double Tavis-Cummings model has been obtained to explain the dynamics of sudden death of entanglement [27]. On the other hand, the entanglement can be quantified by using some different indicators, for example, concurrence [28], the entanglement of formation [29], and negativity [11].

The properties of Jaynes-Cummings model (JCM) were theoretically suggested and studied in the 1960s, and the results were confirmed in practice in the 1980s [30]. Therefore, the JCM is a familiar and important content for researchers in atomic and optical physics. Recently, JCM has been used to describe the evolution of entanglement between atoms and photons by researchers in quantum information science [31]. A thermal JCM and a discussion of the minimal entanglement between a two-level atom and thermal photons were investigated [32]. Moreover, the periods of sudden death and their association with the disentanglement of two separate atoms have been discovered [33]. Furthermore, we are working on our proposal to become one of the important candidates for a way to implement quantum logic in comparing the entanglement periods caused by the interaction of a two- or three-level atom with an ideal field.

It is well known that the formula of the tomographic probability representation is used to describe the quantum states [34]. For the discrete spin observables, the tomographic probability and tomographic entropy have been reconstructed [35]. A comparative study of quantum Fisher information, tomographic entropy, and the von Neumann entropy for a single qubit and optical radiation field in the presence of excited and negative binomial distribution has been introduced [36, 37]. The interaction between a collection of an atomic quantum system and a quantized cavity field has been discussed [9].

The paper is aimed at introducing a new interaction between an optical radiation field and two different dimensional atomic systems, where the two subsystems are two- and three-level atoms. The impact of the initial setting state of the two atoms on the temporal evolution of the physical phenomena is reported. The main task is to investigate the influence of initial atomic angles on some statistical information and quantum correlations of this system. The paper is organized as the following section briefly characterizes the physical Hamiltonian model and obtains the exact solution via the time-dependent Schrödinger equation. Accordingly, the final output atomic state of the two-level and three-level atoms is obtained. Section 3 studies the dynamical behaviour of the atomic statistical inversion influenced by the initial state of the two different dimension atoms. Section 4 dedicates a comparative study of the two quadratures of entropy squeezing for the two atomic subsystems. We introduced the mathematical form of tomographic entropy and its temporal evolution in Section 5. Finally, Section 6 includes our conclusion.

2. The Physical Model

Let us briefly characterize a quantum system consisting of a single-mode cavity field coupled to isolated two- and three-level atoms, where the three-level atom is in Λ configuration (this system is proposed on Figure 1). The total Hamiltonian is expressed as ($\hbar = 1$),

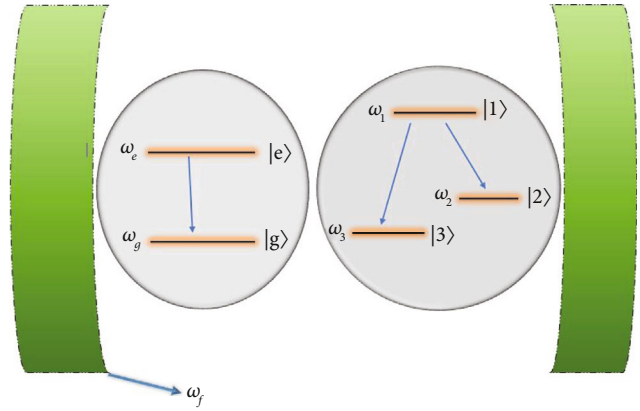

Figure 1: A sketch of two- and three-level atoms interact with a single mode of a quantized cavity field.

$$\mathcal{H} = \omega_f \hat{a}^\dagger \hat{a} + \sum_{\substack{j=e,g \\ 1,2,3}} \omega_j |j\rangle\langle j| + \lambda(\hat{a}|1\rangle\langle 2| + \hat{a}|1\rangle\langle 3| + \hat{a}|e\rangle\langle g| + h.c.), \tag{1}$$

where $\omega_j (j = f, e, g, 1, 2, 3)$ are the field, two-level atom, and three-level atom frequencies, respectively. Also, $\hat{a}$ ($\hat{a}^\dagger$) is the common annihilation (creation) operator of a cavity field. λ denotes the coupling strength of atomic-field interaction.

At any time $t > 0$, we assume that the temporal wave function $|\psi(t)\rangle$ corresponding to the entire Hamiltonian is given by,

$$\begin{aligned} |\psi(t)\rangle = \sum_{n=0}^{\infty} \big(& \mathcal{A}_1(n,t) e^{-i\eta_1 t} |e,1,n\rangle + \mathcal{A}_2(n,t) e^{-i\eta_2 t} |e,2,n+1\rangle \\ & + \mathcal{A}_3(n,t) e^{-i\eta_3 t} |e,3,n+1\rangle + \mathcal{A}_4(n,t) e^{-i\eta_4 t} |g,1,n+1\rangle \\ & + \mathcal{A}_5(n,t) e^{-i\eta_5 t} |g,2,n+2\rangle + \mathcal{A}_6(n,t) e^{-i\eta_6 t} |g,3,n+2\rangle \big), \end{aligned} \tag{2}$$

where $\mathcal{A}_i$ represent the time-dependent probability amplitudes, whilst η_s are defined by,

$$\begin{aligned} \eta_1 &= \omega_e + \omega_1 + n\omega_f, \\ \eta_2 &= \omega_e + \omega_2 + (n+1)\omega_f, \\ \eta_3 &= \omega_e + \omega_3 + (n+1)\omega_f, \\ \eta_4 &= \omega_g + \omega_1 + (n+1)\omega_f, \\ \eta_5 &= \omega_g + \omega_2 + (n+2)\omega_f, \\ \eta_6 &= \omega_g + \omega_3 + (n+2)\omega_f. \end{aligned} \tag{3}$$

Here, the initial state is considered as a separate state (product state), and then the entanglement periods resulting

from the interaction of the field with a two-level atom or a three-level atom are detected via applying the time-dependent Schrödinger equation $i((\partial|\psi(t)\rangle)/\partial t) = \mathscr{H}|\psi(t)\rangle$ [38]. Also, considering the initial state as a linear combination of product states between a superposition of atomic state $|\Xi\rangle$ and the coherent state $|\alpha\rangle$, which is represented by,

$$\begin{aligned}|\psi(0)\rangle &= |\Xi\rangle \otimes |\alpha\rangle \\ &= \left(\cos^2\Theta|e,1\rangle + \cos\Theta\sin\Theta|e,2\rangle + \sin\Theta|e,3\rangle\right) \\ &\quad \otimes \sum_{n=0}^{\infty} Q(n)|n\rangle,\end{aligned} \tag{4}$$

where $Q(n) = e^{-(|\alpha|^2/2)}(\alpha/(n!)^{-1/2})$, while $\Theta \in [0,\pi]$.

The case of resonance is considered for both the two-level atom and the three-level atom. For a two-level atom, the relation between atomic frequencies and field frequency is

$$\omega_e - \omega_g = \omega_f. \tag{5}$$

For a three-level atom, the relationship between the atomic frequencies and the frequency of the field is

$$\begin{aligned}\omega_1 - \omega_2 &= \omega_f, \\ \omega_1 - \omega_3 &= \omega_f.\end{aligned} \tag{6}$$

In the resonance case with the initial states (4), the probability amplitudes in Eq. (2) can be calculated as follows:

$$\begin{aligned}\mathscr{A}_1(n,t) &= \frac{a_1}{2\sqrt{R_1}}\left(X_1^+(n,t) + X_1^-(n,t)\right) \\ &\quad - \frac{i(a2+a3)\nu_1}{\sqrt{2R1}}\left(X_2^+(n,t) + X_2^-(n,t)\right), \\ \mathscr{A}_2(n,t) &= \frac{a_2+a_3}{4\sqrt{R_1}}\left(X_3^+(n,t) + X_3^-(n,t) + 2\sqrt{R_1}\cos(\nu_2 t)\right) \\ &\quad - \frac{ia_1\nu_1}{\sqrt{2R1}}\left(X_2^+(n,t) + X_2^-(n,t)\right), \\ \mathscr{A}_3(n,t) &= \frac{a_2+a_3}{4\sqrt{R_1}}\left(X_3^+(n,t) + X_3^-(n,t) - 2\sqrt{R_1}\cos(\nu_2 t)\right) \\ &\quad - \frac{ia_1\nu_1}{\sqrt{2R1}}\left(X_2^+(n,t) + X_2^-(n,t)\right), \\ \mathscr{A}_4(n,t) &= \frac{a_2+a_3}{\sqrt{R_1}}Y(n,t) - \frac{ia_1\nu_1}{\sqrt{2R1}}\left(X_4^+(n,t) + X_4^-(n,t)\right), \\ \mathscr{A}_5(n,t) &= \frac{2a_1\nu_1\nu_2}{\sqrt{R_1}}Y(n,t) - \frac{i(a_2+a_3)}{2\sqrt{2R_1}}\left(X_4^+(n,t) + X_4^-(n,t)\right) \\ &\quad - \frac{i(a_2-a_3)}{\sqrt{2}}\sin(\nu_2 t), \\ \mathscr{A}_6(n,t) &= \frac{2a_1\nu_1\nu_2}{\sqrt{R_1}}Y(n,t) - \frac{i(a_2+a_3)}{2\sqrt{2R_1}}\left(X_4^+(n,t) + X_4^-(n,t)\right) \\ &\quad + \frac{i(a_2-a_3)}{\sqrt{2}}\sin(\nu_2 t).\end{aligned} \tag{7}$$

Here,

$$\begin{aligned}X_1^{\pm}(n,t) &= \left[\sqrt{R_1} \pm 3\left(\nu_2^2 - \nu_1^2\right)\right]\cos\left(t\sqrt{\frac{\mathscr{D}_{\mp}}{2}}\right), \\ X_2^{\pm}(n,t) &= \left[\frac{\sqrt{R_1} \pm \left(\nu_2^2 + 3\nu_1^2\right)}{\mathscr{D}_{\pm}}\right]\sin\left(t\sqrt{\frac{\mathscr{D}_{\pm}}{2}}\right), \\ X_3^{\pm}(n,t) &= \left[\sqrt{R_1} \pm \left(\nu_2^2 - \nu_1^2\right)\right]\cos\left(t\sqrt{\frac{\mathscr{D}_{\mp}}{2}}\right), \\ X_4^{\pm}(n,t) &= \left[\frac{\sqrt{R_1} \pm \left(3\nu_2^2 + 5\nu_1^2\right)}{\mathscr{D}_{\pm}}\right]\sin\left(t\sqrt{\frac{\mathscr{D}_{\pm}}{2}}\right), \\ Y(n,t) &= \left(\nu_1^2 + \nu_2^2\right)\left(\cos\left(t\sqrt{\frac{\mathscr{D}_{+}}{2}}\right) - \cos\left(t\sqrt{\frac{\mathscr{D}_{-}}{2}}\right)\right),\end{aligned} \tag{8}$$

with

$$\begin{aligned}a_1 &= Q(n)\cos^2\Theta, \\ a_2 &= Q(n)\cos\Theta\sin\Theta, \\ a_3 &= Q(n)\sin\Theta,\end{aligned} \tag{9}$$

where

$$\begin{aligned}R_1 &= 9\left(\nu_1^4 + \nu_2^4\right) + 14\nu_1^2\nu_2^2, \\ \mathscr{D}_{\pm} &= \sqrt{R_1} \pm 3\left(\left(\nu_1^2 + \nu_2^2\right)\right), \\ \nu_{1(2)} &= \lambda\sqrt{n+1(2)}.\end{aligned} \tag{10}$$

By using Eqs. (2) and (7), the final output density operator of the total systems is given by

$$\rho_{\widehat{A,B,f}} = |\psi(t)\rangle\langle\psi(t)|. \tag{11}$$

The main task of this manuscript is to discuss some statistical and dynamical aspects of the reduced density states for the two-level and three-level atoms. To get the reduced density operator, one can trace out the other two subsystems. The reduced density state of the two-level atomic system is defined by $\widehat{\rho}_A = Tr_{B,f}|\psi(t)\rangle\langle\psi(t)|$, which is obtained by

$$\begin{aligned}\widehat{\rho}_A = \sum_{n=0}^{\infty}\Big[&\left(|\mathscr{A}_1(n,t)|^2 + |\mathscr{A}_2(n,t)|^2 + |\mathscr{A}_3(n,t)|^2\right)|e\rangle\langle e| \\ &+ \left(|\mathscr{A}_4(n,t)|^2 + |\mathscr{A}_5(n,t)|^2 + |\mathscr{A}_6(n,t)|^2\right)|g\rangle\langle g| \\ &+ \left(\mathscr{A}_1(n+1,t)\mathscr{A}_4^*(n,t) + \mathscr{A}_2(n+1,t)\mathscr{A}_5^*(n,t)\right. \\ &\left.+ \mathscr{A}_3(n+1,t)\mathscr{A}_6^*(n,t)\right)|e\rangle\langle g| + h.c.\Big].\end{aligned} \tag{12}$$

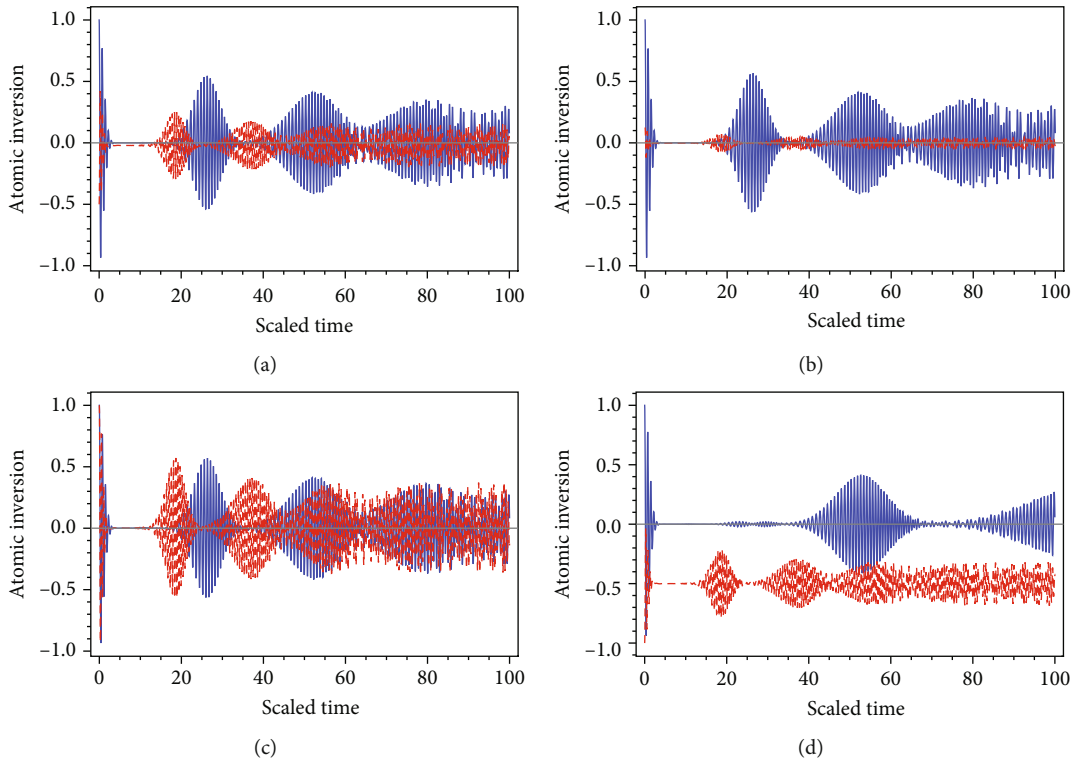

FIGURE 2: The atomic inversion of two-level atom $\mathscr{W}_A(t)$ (blue curve) and three-level atom $\mathscr{W}_B(t)$ (red curve), where (a) $\Theta = \pi/4$, (b) $\Theta = \pi/6$, (c) $\Theta = 0$, and (d) $\Theta = \pi/2$.

Likewise, the reduced density operator of the three-level atom is given by

$$\begin{aligned}\widehat{\rho}_B = \sum_{n=0}^{\infty} \big[&\left(|\mathscr{A}_1(n,t)|^2 + |\mathscr{A}_4(n,t)|^2\right)|1\rangle\langle 1| \\ &+ \left(|\mathscr{A}_2(n,t)|^2 + |\mathscr{A}_5(n,t)|^2\right)|2\rangle\langle 2| \\ &+ \left(|\mathscr{A}_3(n,t)|^2 + |\mathscr{A}_6(n,t)|^2\right)|3\rangle\langle 3| \\ &+ \left(\mathscr{A}_1(n+1,t)\mathscr{A}_2^*(n,t) + \mathscr{A}_4(n+1,t)\mathscr{A}_5^*(n,t)\right)|1\rangle\langle 2| \\ &+ \left(\mathscr{A}_1(n+1,t)\mathscr{A}_3^*(n,t) + \mathscr{A}_4(n+1,t)\right)\mathscr{A}_6^*(n,t)|1\rangle\langle 3| \\ &+ \left(\mathscr{A}_2(n,t)\mathscr{A}_3^*(n,t) + \mathscr{A}_5(n,t)\mathscr{A}_6^*(n,t)\right)|2\rangle\langle 3| + h.c.\big]. \end{aligned} \tag{13}$$

3. Atomic Inversion

Using the statistical population inversion, one can find the possibility of populating an atom in its excited or ground state. The population inversion of the two-level atom can be achieved by using the reduced density state (12) as follows:

$$\begin{aligned}\mathscr{W}_A(t) = &|\mathscr{A}_1(n,t)|^2 + |\mathscr{A}_2(n,t)|^2 + |\mathscr{A}_3(n,t)|^2 - |\mathscr{A}_4(n,t)|^2 \\ &- |\mathscr{A}_5(n,t)|^2 - |\mathscr{A}_6(n,t)|^2. \end{aligned} \tag{14}$$

However, the statistical inversion of the three-level atom via employing the reduced density state (13) reads

$$\begin{aligned}\mathscr{W}_B(t) = &|\mathscr{A}_1(n,t)|^2 - |\mathscr{A}_2(n,t)|^2 - |\mathscr{A}_3(n,t)|^2 + |\mathscr{A}_4(n,t)|^2 \\ &- |\mathscr{A}_5(n,t)|^2 - |\mathscr{A}_6(n,t)|^2. \end{aligned} \tag{15}$$

The influence of the initial atomic state on the statistical population inversion is displayed in Figure 2, where the population of the two- and three-level atoms are shown by the blue and red curves, respectively. By setting the atomic system in the superposition state with $\Theta = \pi/4$, Figure 2(a) shows that the collapse interval of the three-level atom is less than that is depicted for the two-level atom. The oscillation amplitudes of the two-level atom are greater than those displayed in the three-level atomic state. This means that the largest dimension is very sensitive to the field, so the interaction between the two-level atom and the cavity field is more potent. While standing Θ with the value $\pi/6$, Figure 2(b) discloses that the amplitude of the three-level atomic state decreases, and the two-level atom does not change. This illustrates that the three-level atomic state converges to the ground state and that its interaction with the field becomes fragile. By preparing the two atoms in the excited state, Figure 2(c) displays that the two atoms have the same amplitudes. The collapse intervals of the two-level atomic system are longer than that depicted for the three-level atom. If

the higher dimensional atomic state is initially prepared in the ground state and the lower dimensional atomic system at the initial excited state, Figure 2(d) shows that the statistical inversion of the three-level atom always has a negative behaviour, while the collapse interval of the two-level atom increases. From this figure, we can deduce that the initial atomic state plays a central role in the statistical inversion, where the superposition state reduces the efficiency of the interaction between the two atoms and the field. The high atomic dimensionality is very sensitive to the cavity field. The sensitivity of the two-level state of the cavity field becomes fragile if we set the three-level atom in the ground state.

4. Entropy Squeezing

In this section, we shall use the phenomena of entropy squeezing to investigate the information entropy of either the reduced two-level atomic system or the reduced three-level atomic system. It gave the condition of entropy squeezing in x and y directions by [39, 40]

$$\varepsilon_l(\sigma_i) = \exp\left[H_l(\sigma_i)\right] - \frac{\gamma}{\sqrt{\left|\exp\left[H_l(\sigma_z)\right]\right|}} < 0, \quad l = A, B, \text{and } i = x, y, \tag{16}$$

where the parameter γ equals 2 and $2\sqrt{2}$ for two and three-level atom, respectively, and $H_l(\sigma_i)$ are the observable Shannon information entropics with $H_l(\sigma_i) = -\sum_{n=j}^{N} \mathscr{P}_j^l(\sigma_i) \ln \mathscr{P}_j^l(\sigma_i)$. For the two-level atom ($N = 2$) the probabilities $\mathscr{P}_j^A(\sigma_i)$ are obtained by

$$\begin{aligned}
&\mathscr{P}_{1,2}^A(\sigma_x) = \frac{1}{2}\left(1 \pm \mathrm{Re}\left[\rho_{12}^A\right]\right), \quad \mathscr{P}_{1,2}^A(\sigma_y) = \frac{1}{2}\left(1 \pm \mathrm{Im}\left[\rho_{12}^A\right]\right),\\
&\mathscr{P}_1^A(\sigma_z) = \rho_{11}^A,\\
&\mathscr{P}_2^A(\sigma_z) = 1 - \rho_{11}^A, \text{with}\\
&\rho_{12}^A = \mathscr{A}_1(n+1,t)\mathscr{A}_4^*(n,t) + \mathscr{A}_2(n+1,t)\mathscr{A}_5^*(n,t) + \mathscr{A}_3(n+1,t)\mathscr{A}_6^*(n,t),\\
&\rho_{11}^A = |\mathscr{A}_1(n,t)|^2 + |\mathscr{A}_2(n,t)|^2 + |\mathscr{A}_3(n,t)|^2.
\end{aligned} \tag{17}$$

However, the probabilities $\mathscr{P}_j^B(\sigma_i)$ of the three-level atomic subsystem ($N = 3$) are computed as follows:

$$\begin{aligned}
&\mathscr{P}_1^B(\sigma_x) = \frac{1}{2}\left(\rho_{11}^B + \rho_{33}^B - 2\,\mathrm{Re}\left[\rho_{13}^B\right]\right),\\
&\mathscr{P}_{2,3}^B(\sigma_x) = \frac{1}{4}\left(1 + \rho_{22}^B \pm 2\,\mathrm{Re}\left[\sqrt{2}\left(\rho_{12}^B + \rho_{23}^B\right) \pm \rho_{13}^B\right]\right)\\
&\mathscr{P}_1^B(\sigma_y) = \frac{1}{2}\left(\rho_{11}^B + \rho_{33}^B + 2\,\mathrm{Re}\left[\rho_{13}^B\right]\right),\\
&\mathscr{P}_{2,3}^B(\sigma_y) = \frac{1}{4}\left(1 + \rho_{22}^B - 2\,\mathrm{Re}\left[\rho_{13}^B\right] \pm 2\sqrt{2}\,\mathrm{Im}\left[\rho_{12}^B + \rho_{23}^B\right]\right),\\
&\mathscr{P}_1^B(\sigma_z) = \rho_{11}^B, \mathscr{P}_2^B(\sigma_z) = \rho_{22}^B, \mathscr{P}_3^B(\sigma_z) = \rho_{33}^B,
\end{aligned} \tag{18}$$

with

$$\begin{aligned}
&\rho_{11}^B = |\mathscr{A}_1(n,t)|^2 + |\mathscr{A}_4(n,t)|^2,\\
&\rho_{12}^B = \mathscr{A}_1(n+1,t)\mathscr{A}_2^*(n,t) + \mathscr{A}_4(n+1,t)\mathscr{A}_5^*(n,t),\\
&\rho_{22}^B = |\mathscr{A}_2(n,t)|^2 + |\mathscr{A}_5(n,t)|^2,\\
&\rho_{13}^B = \mathscr{A}_1(n+1,t)\mathscr{A}_3^*(n,t) + \mathscr{A}_4(n+1,t)\mathscr{A}_6^*(n,t),\\
&\rho_{33}^B = |\mathscr{A}_3(n,t)|^2 + |\mathscr{A}_6(n,t)|^2,\\
&\rho_{23}^B = \mathscr{A}_2(n,t)\mathscr{A}_3^*(n,t) + \mathscr{A}_5(n,t)\mathscr{A}_6^*(n,t).
\end{aligned} \tag{19}$$

The effect of initial atomic setting state of squeezing degree for the first quadrature $\varepsilon_l(\sigma_x)$ is displayed in Figure 3, where we present the two-level atom $\varepsilon_A(\sigma_x)$ in the blue solid curve and the three-level atom $\varepsilon_B(\sigma_x)$ red dash curve. From Figure 3, we remarked that the two-level atom always has no squeezing along the scaled time, where the behaviour of $\varepsilon_A(\sigma_x) > 0$ for different Θ. Squeezing of the three-level atom is depicted with the initial superposition states and the ground state. The entropy squeezing at $\Theta = \pi/3$ is greater than that displayed for $\Theta = \pi/4$, where $\varepsilon_B(\sigma_x) < 0$ always with $\Theta = \pi/3$. For the ground state, we disclose the entropy squeezing for a small period, where $\varepsilon_B(\sigma_x) < 0$ at the scaled time $\lambda t \in [0.05, 0.06]$. Therefore, the superposition state generates large degrees of squeezing for the three-level atom.

On the other hand, Figure 4 shows the general behaviour of the second quadrature $\varepsilon_l(\sigma_y)$. We noticed that the squeezing phenomenon of the two-level atom is generated after the first onset interaction, and it has a symmetric behaviour for different initial states. For the ground state, we disclose the entropy squeezing for a small period, where $\varepsilon_B(\sigma_x) < 0$ at the scaled time $\lambda t \in [0.05, 0.06]$. Therefore, the superposition state generates large degrees of squeezing for the three-level atom. In contrast, the squeezing phenomenon of the three-level atom is dissipated according to the superposition state or the excited state. The reduced three-level atomic state generates a small-scale squeezing when the two-level atom is prepared in an excited state. From Figures 3 and 4, the two quadratures of entropy squeezing $\varepsilon_l(\sigma_x)$ and $\varepsilon_l(\sigma_y)$ are reflected behaviors. The robustness of entropy squeezing for the three-level atom is stronger than the two-level atom.

5. Tomographic Entropy

For the atomic states, we constructed the tomographic entropy to indicate the entanglement of a quantum system.

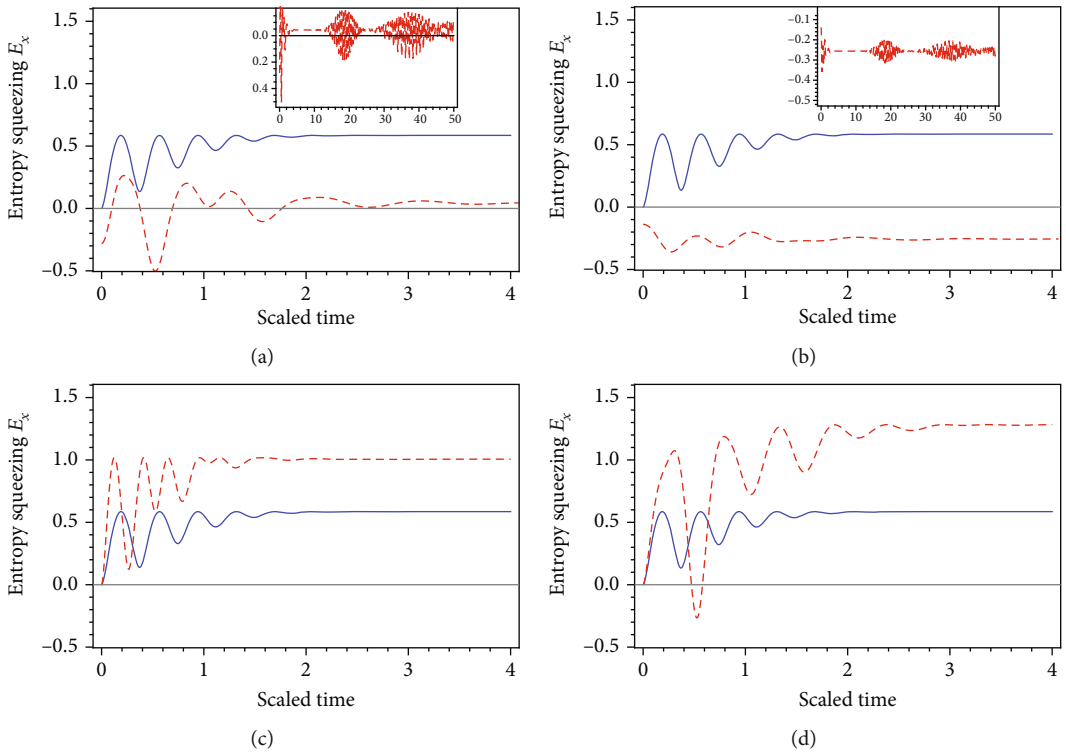

FIGURE 3: (a–d) The entropy squeezing in x direction of two-level atom $\varepsilon_A(\sigma_x)$ (blue curve) and three-level atom $\varepsilon_B(\sigma_x)$ (red curve), with the Θ parameter same as Figure 2.

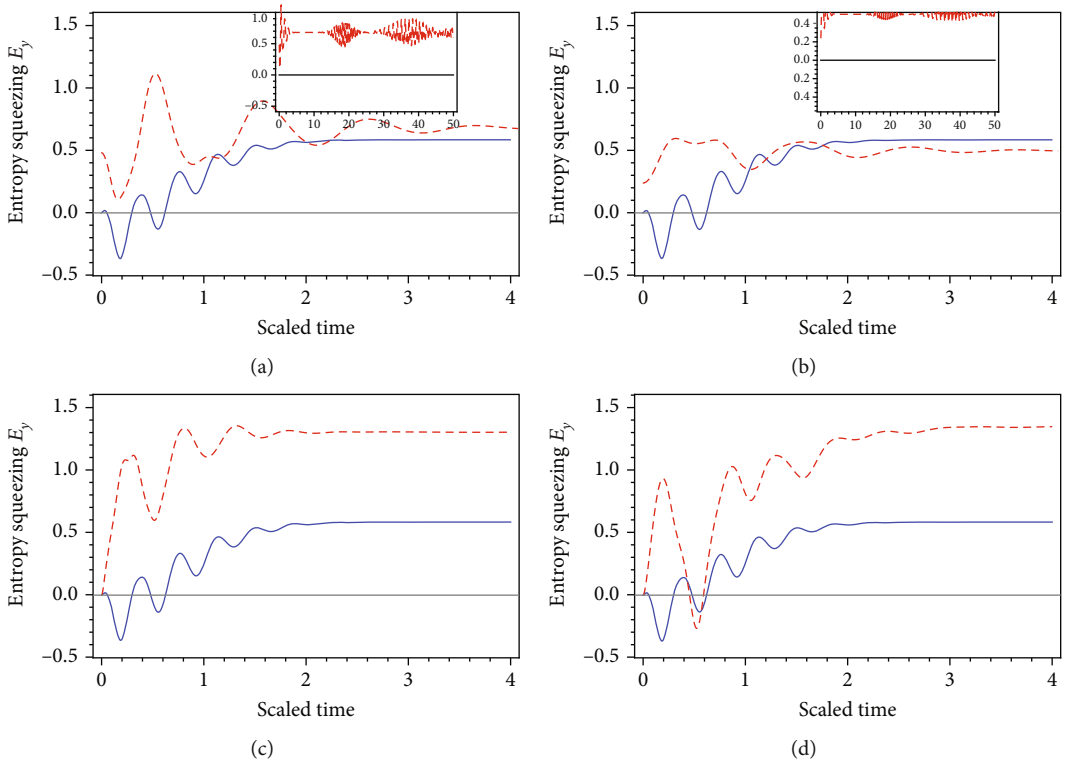

FIGURE 4: (a–d) The entropy squeezing in y direction of two-level atom $\varepsilon_A(\sigma_y)$ (blue curve) and three-level atom $\varepsilon_B(\sigma_y)$ (red curve), with the Θ parameter same as Figure 2.

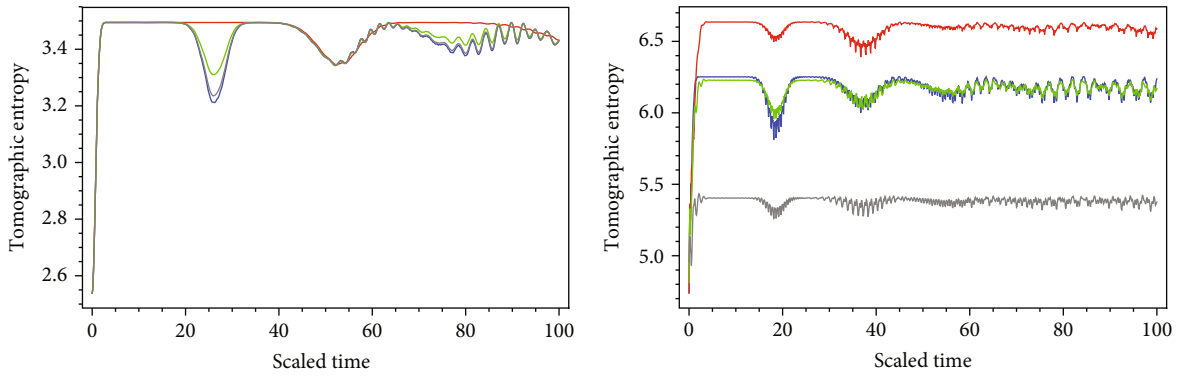

FIGURE 5: The tomographic entropy where $\Theta = 0$ blue curve, $\Theta = \pi/2$ red curve, $\Theta = \pi/3$ green curve, and $\Theta = \pi/4$ gray curve. (a) $\mathcal{T}_A(\alpha, \beta)$ two-level atom. (b) $\mathcal{T}_B(\alpha, \beta)$ three-level atom.

The spin tomogram entropy of an arbitrary spin-j is expressed by [35]

$$\mathcal{T}(\alpha, \beta) = \sqrt{\frac{2j+1}{4\pi}} \int_0^{2\pi} \int_0^{\pi} \sum_{m=-j}^{j} - \mathcal{Q}_m(\alpha, \beta) \ln \mathcal{Q}_m(\alpha, \beta) \sin\alpha \, d\alpha \, d\beta, \tag{20}$$

where $\mathcal{Q}_i(\alpha, \beta)$ represent the generic spin tomograms [35]. For the reduced two-level atom ($j = 1/2$), the tomographic entropy is given by [37]

$$\mathcal{T}_A(\alpha, \beta) = \sqrt{\frac{1}{2\pi}} \int_0^{2\pi} \int_0^{\pi} \sum_{m=1}^{2} - \mathcal{Q}_m^A(\alpha, \beta) \ln \mathcal{Q}_m^A(\alpha, \beta) \sin\alpha \, d\alpha \, d\beta. \tag{21}$$

Here,

$$\mathcal{Q}_1^A(\alpha, \beta) = \frac{1}{2} + \left(\rho_{11}^A - \frac{1}{2}\right) \cos\alpha + \sin\alpha \, \mathrm{Re}\left[\rho_{12}^A e^{i\beta}\right],$$
$$\mathcal{Q}_2^A(\alpha, \beta) = \frac{1}{2} + \left(\frac{1}{2} - \rho_{11}^A\right) \cos\alpha - \sin\alpha \, \mathrm{Re}\left[\rho_{12}^A e^{i\beta}\right], \tag{22}$$

where ρ_{ij}^A are defined in Eq. (17). Likewise, the tomographic entropy of the reduced three-level system ($j = 1$) is computed as [35]

$$\mathcal{T}_B(\alpha, \beta) = \sqrt{\frac{3}{4\pi}} \int_0^{2\pi} \int_0^{\pi} \sum_{m=0}^{3} - \mathcal{Q}_m^B(\alpha, \beta) \ln \mathcal{Q}_m^B(\alpha, \beta) \sin\alpha \, d\alpha \, d\beta, \tag{23}$$

with the generic spin,

$$\begin{aligned}
\mathcal{Q}_1^B(\alpha, \beta) &= \rho_{11}^B \cos^4\frac{\alpha}{2} + \frac{\rho_{22}^B}{2} \sin^2\alpha + \rho_{33}^B \sin^4\frac{\alpha}{2} \\
&+ \frac{\sin^2\alpha}{2} \mathrm{Re}\left[\rho_{13}^B \exp\left[2i\beta\right]\right] \\
&+ \sqrt{2} \sin\alpha \left(\cos^2\frac{\alpha}{2} \mathrm{Re}\left[\rho_{12}^B \exp\left[i\beta\right]\right]\right. \\
&\left. + \sin^2\frac{\alpha}{2} \mathrm{Re}\left[\rho_{23}^B \exp\left[i\beta\right]\right]\right), \\
\mathcal{Q}_2^B(\alpha, \beta) &= \frac{\rho_{11}^B}{2} \sin^2\frac{\alpha}{2} + \rho_{11}^B \cos^2\alpha + \frac{\rho_{33}^B}{2} \sin^2\frac{\alpha}{2} \\
&- \sin^2\alpha \, \mathrm{Re}\left[\rho_{13}^B \exp\left[2i\beta\right]\right] \\
&- \frac{1}{\sqrt{2}} \sin 2\alpha \left(\mathrm{Re}\left[\rho_{12}^B \exp\left[i\beta\right]\right] - \mathrm{Re}\left[\rho_{23}^B \exp\left[i\beta\right]\right]\right), \\
\mathcal{Q}_3^B(\alpha, \beta) &= \rho_{11}^B \sin^4\frac{\alpha}{2} + \frac{\rho_{22}^B}{2} \sin^2\alpha + \rho_{33}^B \cos^4\frac{\alpha}{2} \\
&+ \frac{\sin^2\alpha}{2} \mathrm{Re}\left[\rho_{13}^B \exp\left[2i\beta\right]\right] \\
&- \sqrt{2} \sin\alpha \left(\sin^2\frac{\alpha}{2} \mathrm{Re}\left[\rho_{12}^B \exp\left[i\beta\right]\right]\right. \\
&\left. + \cos^2\frac{\alpha}{2} \mathrm{Re}\left[\rho_{23}^B \exp\left[i\beta\right]\right]\right).
\end{aligned} \tag{24}$$

The tomographic entropy of the two- and three-level atomic systems is displayed in Figures 5(a) and 5(b), respectively. For the two-level state, the initial atomic state has no clear influence on the tomographic entropy. The function $\mathcal{T}_A(\alpha, \beta)$ osculates between 2.55 and 3.5. The maximum bounds when the initial two atoms are prepared in the excited state are less than that shown in the superposition state. The upper bounds of the function $\mathcal{T}_A(\alpha, \beta)$ increase when the first atom is excited and the second in the ground state. For the three-level atomic state, Figure 5(b) shows that the parameter Θ plays a controlled role in tomographic entropy. The lower bounds of the function $\mathcal{T}_B(\alpha, \beta)$ at $\Theta = 0, \pi/2$ exit 4.7, while the upper bounds at $\Theta = 0$ are greater than that are displayed at $\Theta = \pi/2$.

Moreover, at superposition states with $\Theta = \pi/4, \pi/3$, the lower and upper bounds of the tomographic entropy are convergent. The two-level atom is exchanged from a separable state into a partial (maximum) entangled state. However, the initial product state between the excited and ground state generates a maximally entangled state of the three-level atom.

6. Summary

In this paper, we have introduced a physical Hamiltonian comprising of an isolated two- and three-level atoms which are interacting locally with a single mode of a quantized cavity field. The exact solution of this system under different initial setting states by using the time-dependent Schrödinger picture is obtained. The temporal evolution of the statistical atomic inversion, entropy squeezing, and tomographic entropy of the two- and the three-level atoms are investigated. We remarked that the initial state has an active role in the dynamics of the statistical atomic inversion, where the superposition state suppresses the efficacy of the interaction between the atom and the field. The high-dimensional atomic system is sensitive to the cavity field. However, the sensitivity between the two-level state and the cavity field become more fragile if we set the three-level atom in the ground state. Also, the robustness of the entropy squeezing depends on the dimension of the atomic system, where the three-level state is stronger than the two-level atom. The general behaviours of the two quadratures of the entropy squeezing are reflected. By controlling the initial setting states, one can increase/suppress the temporal evolution of the tomographic entropy induced by the influence of the separability in the quantum system.

Data Availability

The data used is generated from the models presented in the manuscript.

Conflicts of Interest

The authors declare that they have no conflicts of interest.

Acknowledgments

This research was supported by Taif University, Saudi Arabia, supporting project number TURSP-2020/17.

References

[1] E. T. Jaynes and F. W. Cummings, "Comparison of quantum and semiclassical radiation theories with application to the beam maser," *Proceedings of the IEEE*, vol. 51, no. 1, pp. 89–109, 1963.

[2] M. Sebawe Abdalla, M. M. A. Ahmed, and A.-S. F. Obada, "Dynamics of a non-linear Jaynes-Cummings model," *Physica A: Statistical Mechanics and its Applications*, vol. 162, no. 2, pp. 215–240, 1990.

[3] B. M. Rodríguez-Lara, F. Soto-Eguibar, A. Z. Cárdenas, and H. M. Moya-Cessa, "A classical simulation of nonlinear Jaynes–Cummings and Rabi models in photonic lattices," *Optics Express*, vol. 21, no. 10, pp. 12888–12898, 2013.

[4] J. Braumüller, M. Marthaler, A. Schneider et al., "Analog quantum simulation of the Rabi model in the ultra-strong coupling regime," *Nature communications*, vol. 8, no. 1, pp. 1–8, 2017.

[5] W. Bruce, "The Jaynes-Cummings model," *Journal of Modern Optics*, vol. 40, no. 7, pp. 1195–1238, 1993.

[6] F. Jahanbakhsh and M. K. Tavassoly, "The field-field and dipole-dipole coupling effects on the entanglement of the interaction between two qutrits with a two-mode field," *Modern Physics Letters A*, vol. 35, no. 22, article 2050183, 2020.

[7] L.-J. Feng, Y. Yu, and H.-X. Dong, "Enhancing cross-Kerr coupling via mechanical parametric amplification," *Optics Express*, vol. 29, no. 18, pp. 28835–28842, 2021.

[8] G. Sadiek, E. I. Lashin, and M. S. Abdalla, "Entanglement of a two-qubit system with anisotropic XYZ exchange coupling in a nonuniform time-dependent external magnetic field," *Physica B*, vol. 404, no. 12-13, pp. 1719–1728, 2009.

[9] M. Sebawe, "Statistical properties of multiphoton time-dependent three-boson coupled oscillators," *Josa B*, vol. 23, no. 6, pp. 1146–1160, 2006.

[10] M. Sebawe Abdalla, M. M. A. Ahmed, E. M. Khalil, and A.-S. F. Obada, "The interaction between a single two-level atom coupled to an N-level quantum system through three couplings," *Annals of Physics*, vol. 364, pp. 168–181, 2016.

[11] R. Horodecki, P. Horodecki, M. Horodecki, and K. Horodecki, "Quantum entanglement," *Reviews of Modern Physics*, vol. 81, no. 2, pp. 865–942, 2009.

[12] G. Sadiek, W. Al-Drees, and S. Abdallah, "Manipulating entanglement sudden death in two coupled two-level atoms interacting off-resonance with a radiation field: an exact treatment," *Optics express*, vol. 27, no. 23, pp. 33799–33825, 2019.

[13] M. Ramzan and M. K. Khan, "Decoherence and entanglement degradation of a qubit-qutrit system in non-inertial frames," *Quantum Information Processing*, vol. 11, no. 2, pp. 443–454, 2012.

[14] N. Metwally, "Entanglement routers via a wireless quantum network based on arbitrary two qubit systems," *Physica Scripta*, vol. 89, no. 12, article 125103, 2014.

[15] N. Metwally, "Enhancing entanglement, local and non-local information of accelerated two qubit and two-qutrit systems via weak-reverse measurements," *EPL*, vol. 116, no. 6, article 60006, 2017.

[16] I. Sainz and G. Björk, "Entanglement invariant for the double Jaynes–Cummings model," *Physical Review A*, vol. 76, no. 4, article 042313, 2007.

[17] S. Jamal, "Entanglement dynamics of three and four level atomic system under Stark effect and Kerr-like medium," *Quantum reports*, vol. 1, no. 1, pp. 23–36, 2019.

[18] E. M. Khalil, S. Abdalla, and A.-S. F. Obada, "Pair entanglement of two-level atoms in the presence of a nondegenerate parametric amplifier," *Journal of Physics B: Atomic, Molecular and Optical Physics*, vol. 43, no. 9, article 095507, 2010.

[19] Q. Liao and G. He, "Maximal entanglement and switch squeezing with atom coupled to cavity field and graphene membrane," *Quantum Information Processing*, vol. 19, no. 3, pp. 1–15, 2020.

[20] M. F. Alotibi, E. M. Khalil, S. Abdel-Khalek, M. Y. Abd-Rabbou, and M. Omri, "Effects of the vibrating graphene

membrane and the driven classical field on an atomic system coupled to a cavity field," *Results in Physics*, vol. 31, article 105012, 2021.

[21] M. S. Abdalla, E. M. Khalil, and A.-S. F. Obada, "Exact treatment of the Jaynes-Cummings model under the action of an external classical field," *Annals of physics*, vol. 326, no. 9, pp. 2486–2498, 2011.

[22] M. Y. Abd-Rabbou, E. M. Khalil, M. M. A. Ahmed, and A. S. F. Obada, "External classical field and damping effects on a moving two level atom in a cavity field interaction with Kerr-like medium," *International Journal of Theoretical Physics*, vol. 58, no. 12, pp. 4012–4024, 2019.

[23] A.-S. F. Obada, F. A. Mohammed, H. A. Hessian, and A.-B. A. Mohamed, "Entropies and entanglement for initial mixed state in the multi-quanta JC model with the Stark shift and Kerr-like medium," *International Journal of Theoretical Physics*, vol. 46, no. 4, pp. 1027–1044, 2007.

[24] N. Metwally, "Dynamics of information in the presence of deformation," *International Journal of Quantum Information*, vol. 9, no. 3, pp. 937–946, 2011.

[25] H.-M. Zou and M.-F. Fang, "Analytical solution and entanglement swapping of a double Jaynes–Cummings model in non-Markovian environments," *Quantum Information Processing*, vol. 14, no. 7, pp. 2673–2686, 2015.

[26] Q. Xie and M.-F. Fang, "Entanglement dynamics of atoms in double Jaynes–Cummings models with Kerr medium," *Communications in Theoretical Physics*, vol. 54, no. 5, pp. 840–844, 2010.

[27] Z.-X. Man, Y.-J. Xia, and N. B. An, "Entanglement dynamics for the double Tavis-Cummings model," *The European Physical Journal D*, vol. 53, no. 2, pp. 229–236, 2009.

[28] H. Fan, K. Matsumoto, and H. Imai, "Quantify entanglement by concurrence hierarchy," *Journal of Physics A: Mathematical and General*, vol. 36, no. 14, pp. 4151–4158, 2003.

[29] K. William, "Entanglement of formation of an arbitrary state of two qubits," *Physical Review Letters*, vol. 80, no. 10, pp. 2245–2248, 1998.

[30] G. Rempe, H. Walther, and N. Klein, "Observation of quantum collapse and revival in a one-atom maser," *Physical review letters*, vol. 58, no. 4, pp. 353–356, 1987.

[31] S. Bose, P. L. Fuentes-Guridi, P. L. Knight, and V. Vedral, "Subsystem purity as an enforcer of entanglement," *Physical Review Letters*, vol. 87, no. 5, article 050401, 2001.

[32] H. Azuma, "Dynamics of the Bloch vector in the thermal Jaynes-Cummings model," *Physical Review A*, vol. 77, no. 6, article 063820, 2008.

[33] T. Yu and J. H. Eberly, "Quantum open system theory: bipartite aspects," *Physical review letters*, vol. 97, no. 14, article 140403, 2006.

[34] A. B. Klimov, O. V. Man'ko, V. I. Man'ko, Y. F. Smirnov, and V. N. Tolstoy, "Tomographic representation of spin and quark states," *Journal of Physics A: Mathematical and General*, vol. 35, no. 29, pp. 6101–6123, 2002.

[35] N. Vladimir, "Tomographic characteristics of spin states," *Research*, vol. 27, no. 2, pp. 132–166, 2006.

[36] A. Almarashi, A. Algarni, S. Abdel-Khalek, and H. K. T. Ng, "Quantum Fisher information and tomographic entropy of a single qubit in excited binomial and negative binomial distributions," *Journal Russian Laser Research*, vol. 40, no. 4, pp. 313–320, 2019.

[37] A. Almarashi, A. Algarni, S. Abdel-Khalek, G. A. Abd-Elmougod, and M. Z. Raqab, "Quantum extropy and statistical properties of the radiation field for photonic binomial and even binomial distributions," *Journal of Russian Laser Research*, vol. 41, no. 4, pp. 334–343, 2020.

[38] W. H. Louisell, *Quantum Statistical Properties of Radiation*, John Wiley and Sons, Inc., New York, 1973.

[39] M.-F. Fang, P. Zhou, and S. Swain, "Entropy squeezing for a two-level atom," *Journal of Modern Optics*, vol. 47, no. 6, pp. 1043–1053, 2000.

[40] A.-S. F. Obada, N. A. Alshehri, E. M. Khalil, S. Abdel-Khalek, and H. F. Habeba, "Entropy squeezing and atomic Wehrl density for the interaction between SU(1,1) Lie algebra and a three-level atom in presence of laser field," *Results in Physics*, vol. 30, article 104759, 2021.